

الكشف عن التوافقيات الفضائية من المحرك التعريفي القطب المظلمة

أديم دالكالي* ومحمد أكيبا**

* الهندسة الكهربائية والإلكترونيات، جامعة كارابوك، كارابوك، 78050، تركيا

** هندسة الحاسوب، جامعة كارابوك، كارابوك، 78050، تركيا

الخلاصة

وفي كثير من الحالات، يكون لمحركات الحث القطبية المظلمة ثغرات هواء متغيرة، وبسبب هذا تكون أشكال الموجة الكثافة للتدفق الهبوطي للهواء بعيدة جدا عن التوزيع الجيبي. ويساعد استخدام الفوارق الهوائية المتغيرة في المحركات القطبية المظلمة في عزم الدوران بدءا بإحداث عنصر عزم الدوران المتردد. ومع ذلك، فإن الفجوة الجوية المتغيرة تقدم مكونات مذبذبة إضافية للتوافق في أشكال موجات الكثافة للتدفق الهوائي. في هذه الدراسة، تم الكشف عن توافقيات الفضاء من محرك تحريض القطب المظلمة. لتكون قادرة على الكشف عن توافقيات الفضاء، وقد تم إنتاج الدوار للمحرك بطريقة لم يصب فيها الألومنيوم ولم يتم إدراج حلقات قصيرة كهربائية في الدوار. لفائف السلك المعروف عددها تم ادراجها إلى الدوار، وقد تم تطبيق الجهد تصنيفا إلى الجزء الثابت وموقف الدوار وقد تم تنويع مع زاوية الكهربائية خطوة من 3.60 مع مساعدة من خطوة المحرك. وقد تم تحديد الحث المتبادل بين الموالي والدوار من خلال قراءة الجهد الناجم عبر اللفائف. وقد تم إخضاع موجة الحث المتبادل المتحقق لتحليل (Fourier) المنفصل. ونتيجة للتحليلات، فقد لوحظ أن التوافقيات 3 و 5 و 7 خاصة كبيرة جدا. التوافقيات الأخرى تصل إلى الرتبة 13 هي فوق 1٪ من المكون الأساسي والرتبة 15 والتوافقيات اللاحقة يقل أقل من 0.8٪ من المكون الأساسي لشكل موجة كثافة تدفق الهواء. لذلك، لتحليل أداء معقول إلى حد معقول من هذه الآلات على الأقل التوافقيات 3، 5 و 7 ينبغي اخذها في الاعتبار.

Detection of the space harmonics of the shaded pole induction motor

Adem Dalcalı* and Mehmet Akbaba**

**Electrical-Electronics Engineering, Karabuk University, Karabuk, 78050, Turkey*

***Computer Engineering, Karabuk University, Karabuk, 78050, Turkey*

Corresponding Author: ademdalcali@karabuk.edu.tr

ABSTRACT

In many cases, shaded pole induction motors have variable air gaps, and because of this, their air-gap flux density waveforms are too far from a sinusoidal distribution. Utilizing of variable air-gap in shaded pole motors contributes to the starting torque by inducing reluctance torque component. However, variable air-gap introduces additional harmonic components in the air-gap flux density waveforms. In this study, detection of the space harmonics of the shaded pole induction motor has been realized. To be able to detect the space harmonics, the rotor of the motor has been produced in a way that aluminum has not been cast, and the short circuit rings of the rotor has have not been inserted. A search-coil whose number of turns is known has been wound to the rotor, rated voltage has been applied to the stator, and the position of the rotor has been varied with a step electrical angle of 3.6° with the help of a step motor. The mutual inductance between the stator and rotor has been determined by reading the voltage induced across the search-coil. The attained mutual inductance waveform has been subjected to Discrete Fourier analysis. From the analyses, it has been observed that especially the 3rd, 5th, and 7th harmonics, especially, are very significant. Other harmonics up to 13th are above 1% of the fundamental component, and the 15th and subsequent harmonics decreases below 0.8% of the fundamental component of the air-gap flux density waveform. Therefore, for a reasonably accurate performance, an analysis of this these machines, at least 3rd, 5th, and 7th harmonics, should be considered.

Keywords: Discrete Fourier analysis; Mutual inductance; Shaded pole motor; Space harmonics.

INTRODUCTION

Shaded pole induction motors (SPIMs) are widely used especially in the ventilation systems in the industry because of their advantages such as their robust structures, and easiness in maintenance and production, and direct feeding from single single-phase supply without any requirement for from the driver. However, the formation of elliptic rotating magnetic field in SPIM makes the analysis of the machine difficult. There is no standard procedure in the analysis of such kinds of motors, and their mathematical modeling, and in the realization of motor performance analyses (Sarac & Stefanov, 2011; Dehkordi, 2015). For this reason, there are very few studies conducted on these kinds of motors (Kentli, 2009). Despite this, as much as 10 million pieces per year of these motors are produced in Europe alone. Single-phase motors with capacitor are produced as much as 700-800 thousand pieces in Europe per year. Other alternative efficient motors are produced as much as 100 thousand pieces per year in Europe (Karmakar *et al.*, 2013).

Ozcelik *et al.*, have expressed that the shaded pole motors are preferred due to their simple

structure especially in the household electrical appliances in low torque and low power applications. In their study, the performance of brushless DC motor with capacitor and, single-phase and permanent magnet has been compared. From the tests results, it has been shown that the shaded pole motor is acceptable in terms of meeting the load torque and it is also superior in terms of cost, but brushless DC motor is superior in terms of efficiency (Ozcelik *et al.*, 2014). Sarac has aimed to at developing the performance of shaded pole motor by using genetic algorithm. Two motor models have been determined; the torque has been determined as the target function in the first motor and, efficiency has been determined as the target function in the second motor, and the enhancement of torque and efficiency has have been provided (Sarac *et al.*, 2005). Sarac *et al.* have designed three different types of motors in their other studies, and an increase in the efficiency has been reported by determining the stator winding current density, air-gap flux density, rotor skew, and stator pole width as the variables (Sarac *et al.*, 2010). Goa has checked the speed of the shaded pole motor used in the cooling fan systems by using d-q axis model (Gao *et al.*, 2005). Ojaghi and Daliri have attained the dynamic model of the shaded pole motor and ensured the realization of performance analyses under different operational conditions in the design and implementation stages (Ojaghi & Daliri, 2015). In their study, in which small electrical motors have been examined, Hajek *et al.* has detected that the magnetic fields under the poles of the shaded pole motors are not sinusoidal; rather, they are in distorted rectangular form and they have very high 3rd harmonic component (Hajek *et al.*, 2015). In this study, a shaded pole motor produced by Faneks Fan (model F4KGM25-01), which has the rating of the 4pole, 1305 rpm, and 15 W, is used. Harmonics analysis of this motor is made by first obtaining the air-gap flux density waveform and then performing the Discrete Fourier analysis of this waveform.

SHADED POLE INDUCTION MOTORS

Shaded pole induction motors are preferred due to their properties such as simple production and easiness in maintenance among the single-phased induction motors. These motors could directly operate from a single-phased network. They are preferred more when compared to other single-phase motors in the places requiring power less than 150W and they have a wide application area such as the fan applications, small household appliances, and toys (Akbaba & Fakhro, 1992a; Akbaba & Fakhro, 1992b; Ozcelik *et al.*, 2014). Despite their simple structure, the performance analysis of these motors are is very difficult, and there isn't any standard equivalent circuit or method of analysis for estimating their performance accurately. This is mainly due to the formation of elliptical magnetic rotating field with rich harmonics (Dalcalı & Akbaba, 2016). The properties of the motor used in this study are given in Table 1 and structure of the motor used is shown in Figure 1.

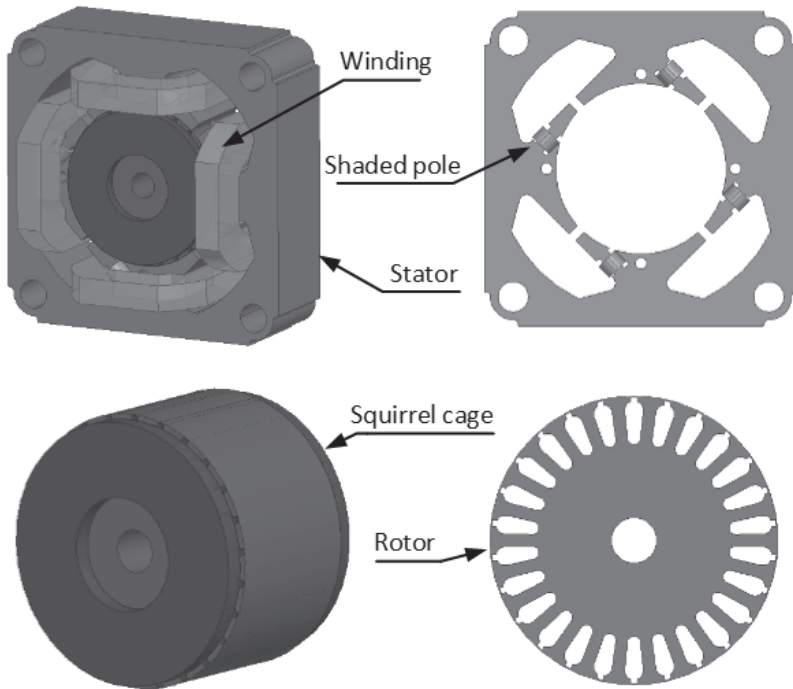


Fig. 1. Structure of shaded pole motor.

Table 1. The properties of the motor.

| Property | Value | Property | Value |
|-------------------|-------|------------------------------|----------|
| Power(W) | 15 | Rotor diameter (mm) | 22 |
| Voltage (V) | 220 | Core size (mm) | 82x82x25 |
| Frequency (Hz) | 50 | Rotor steel sheet material | M270-50A |
| Number of poles | 4 | Stator steel sheet material | M270-50A |
| Rotor speed (rpm) | 1305 | Number of main winding turns | 580 |
| Rated current (A) | 0.375 | Number of rotor slots | 26 |

Determination of the Stator-Rotor Mutual Inductance While Shading Rings Are Absent

Stator-rotor mutual inductance is determined by measuring the voltage induced in search-coil placed into two neighbor slots and two teeth between these two slots in the rotor, in which the rotor cage and end rings have not been inserted. The motor produced without any cast of aluminum and the stator produced without the insertion of short circuit rings (shading rings) are given in Figure 2. The aluminum casted and shading rings inserted version of the same motor has also been produced, and the performance tests have been conducted on this motor.

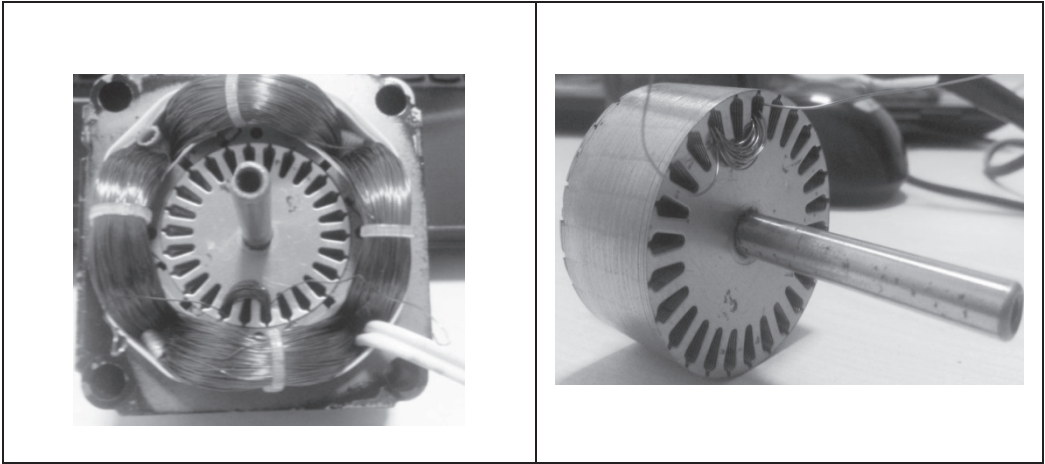


Fig. 2. The motor and rotor used in the experiment.

A search-coil whose number of turns is 40 has been wound on a rotor teeth between two neighboring empty rotor slots for the of measuring the mutual inductance between the stator winding and a single rotor loop that is composed of two neighbor slots and a teeth between these two slots. A known stator current I_a have has been applied from the stator winding, and the voltage E induced in the search-coil have has been measured. Out of these measurements, the mutual inductance between the stator winding and a single rotor loop has been determined from the Equation (1) for a certain rotor position:

$$M_{r,s} = \frac{E}{2\pi \cdot f \cdot N \cdot I_a} \quad (1)$$

In Eequation 1, N is the number of turns of the stator's main winding and E is the voltage induced on search-coil at a rotor position θ . Variation of the mutual inductance against rotor position has been obtained by rotating the rotor with certain angles and conducting measurements in each position:

$$M_{r,s}(\theta) = f(\theta) \quad (2)$$

The testing apparatus in Figure 3 has been established for the purpose of obtaining the inductances with certain steps without distorting the value of the air-gap. In the apparatus, a step motor with 200 steps has been coupled with shaded pole motor. The step motor operates with 1.8° mechanical angle and 3.6° electrical angle precision. The step motor has been triggered with the interval of 10 seconds with the help of a microcontroller, and the search-coil voltage and stator winding current have been recorded for each rotor position.

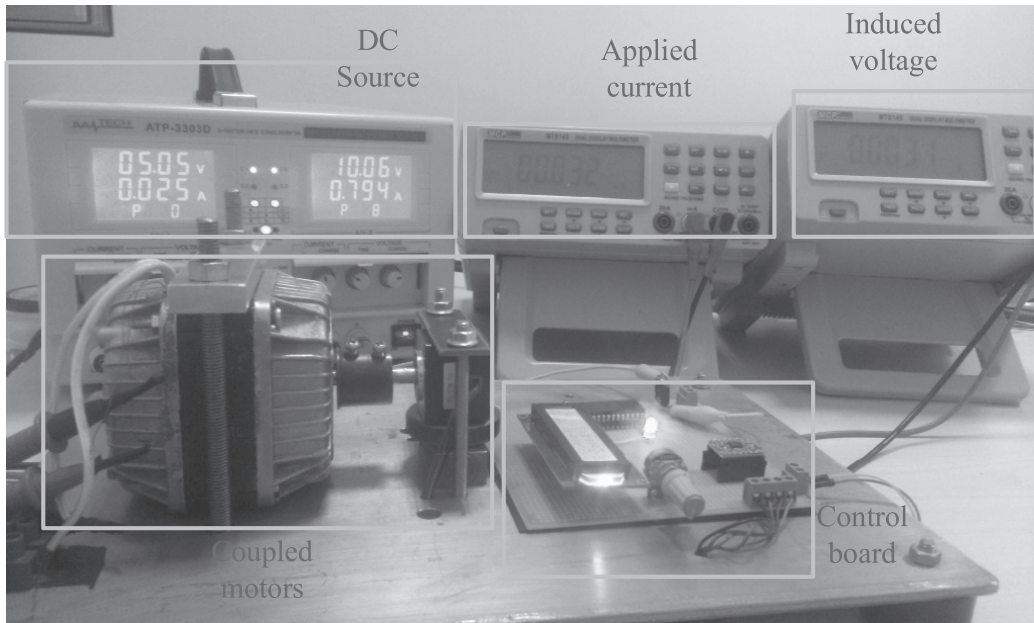


Fig. 3. Experimental setup.

The flow diagram of the established system is given in Figure 4. Regarding the flow diagram, firstly, the adjustments of the input-output pins of the microcontrollers and the assignments of the variables have been adjusted. From this, the rotor position information has been observed with the help of LCD. The microprocessor controlling the system ensures the rotation of the motor for a step per each 10 seconds and, therefore, ensures the motor to change its (electrical) position by 3.6 .

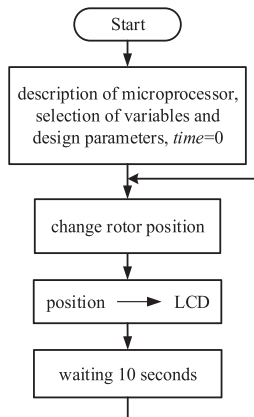


Fig. 4. Flow diagram.

From the test results the realized tests and associated simple calculations, the mutual inductance waveform obtained for 360° electrical rotation of the rotor position is given in Figure 5.

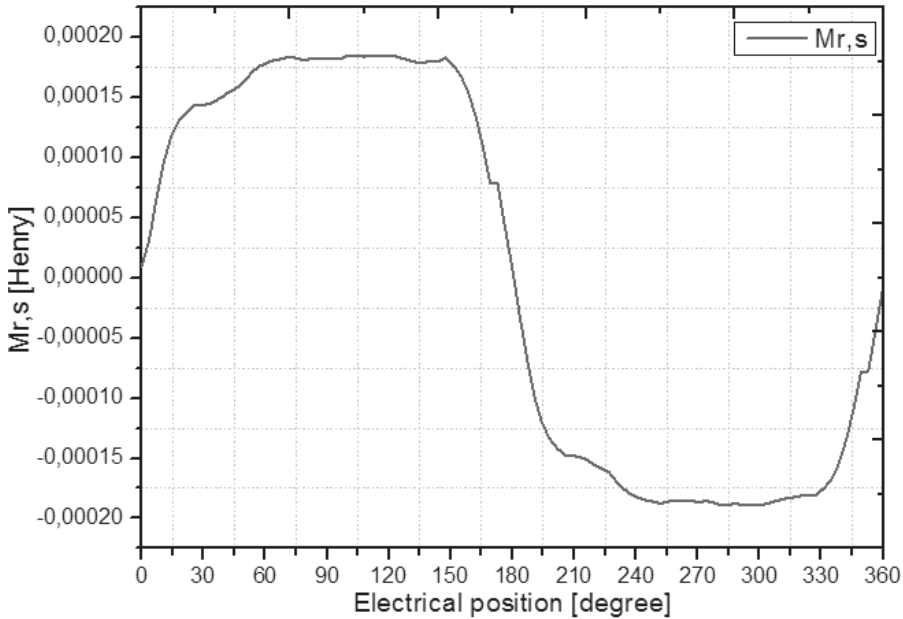


Fig. 5. Variation of the mutual inductance versus rotor position.

THE CONCEPT OF HARMONICS IN SPIM

In most cases, the frequencies of the harmonics in the electrical energy system are the full multiples of the fundamental frequency and they cause to distortions in the induced voltage and adversely affect the performance. Two types of harmonic concepts are defined in the electrical machines. The first one of them is the time harmonic stemming from the distortion of the source voltage from the sinus shape, and the second one is the space harmonic caused by distortion mainly in the air-gap flux or flux density due to non-uniform geometry of the machine air-gap. The space harmonics result in different frequency components besides fundamental component that are observed in the magnetomotive force even when the machine is fed by with sinusoidal voltage. These harmonic components cause to vibrations and noise during the running of the motor (Bayram & Mergen, 2009; Kocabaş & Mergen, 2006). In addition, these harmonics significantly decrease the important performance parameters of the motor such as efficiency, power factor, and torque. Therefore, conducting Discrete Fourier analysis of the air-gap flux density provides information regarding the effect of space harmonics on the performance of the motor. The determination of the harmonic spectrums of the non-sinusoidal waves could be graphically realized via the Discrete Fourier equations. In this method, the non-sinusoidal wave is piecewise linearized with equal small intervals and the average value of each one of them is determined. The attained mutual inductance waveform between stator-rotor could be expressed with the Discrete Fourier series mathematically as in Equation (3) (Kocatepe *et al.*, 2003; Liang *et al.*, 2016; Pop *et al.*, 2013):

$$M_{r,s}(\theta) = A_0 + \sum_{n=1}^{\infty} (A_n \cos n\theta + B_n \sin n\theta) \quad (3)$$

In the above equation, $M_{r,s}$ is the stator-rotor mutual inductance, θ is the rotor position angle expressed in electrical degree, A_0 is the DC component or mean value, n is the harmonic order, A_n and B_n are the Fourier coefficients of the n th order harmonics and n is the harmonic order. Discrete Fourier coefficients could be expressed by using Equations (4) and (5):

$$A_n = \frac{2}{m} \sum_{k=1}^m (y_k \cos(n\theta_k)) \tag{4}$$

and

$$B_n = \frac{2}{m} \sum_{k=1}^m (y_k \sin(n\theta_k)) \tag{5}$$

In the above equations, m represents the number of intervals in one period of the mutual inductance wave, θ_k represents the central position angle of each interval ($k=1,2,\dots,m$), y_k represents the amplitude of the inductance value corresponding to each θ_k , and n represents the harmonic order. Using Fourier coefficients, the mutual inductance as a function of the rotor position could be expressed as in Equation (6):

$$M_{r,s}(\theta) = A_1 \cdot \sin \theta + \dots + A_n \cdot \sin(n\theta) + B_1 \cdot \cos \theta + \dots + B_n \cdot \sin(n\theta) \tag{6}$$

Stator-rotor mutual inductance waveform obtained from the experiments has been examined until 51st harmonic by conducting Discrete Fourier analysis. The harmonic spectrum until 23rd harmonic is obtained by using Discrete Fourier series method in MATLAB and it is given in Figure 6.

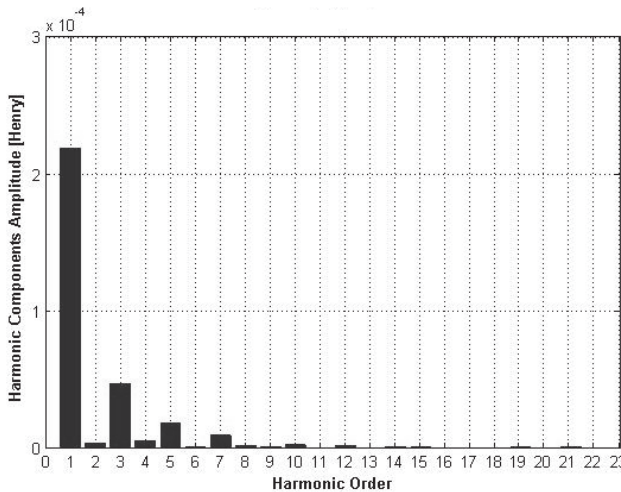


Fig. 6. Harmonic spectrum (1: Fundamental).

When the attained harmonic distribution is examined, it is seen that especially the 3rd harmonic value, especially, is dominant and harmonic orders of 15th and above have negligibly small amplitude (below 0.8%) and they can be ignored. Even harmonics appearing in Figure 6 are due to measurement errors and round-off errors in calculations. The summary of the impacts of the odd harmonics in percentage of the fundamental are given in Table 2. The harmonic amplitudes given in Table 2 are expressed in microhenries. Examination of Table 2 shows that the dominant harmonics are the 3rd, 5th, and 7th harmonics.

Table 2. Percentage harmonic ratios.

| No.n | Harmonic Amplitude (μH) | Angle of the Inductance (degree) | Percentage of Harmonic Ratio | No.n | Harmonic Amplitude (μH) | Angle of the Inductance (degree) | Percentage of Harmonic Ratio |
|------|--------------------------------------|----------------------------------|------------------------------|------|--------------------------------------|----------------------------------|------------------------------|
| 1 | 218.5660 | -2.05 | 100 % | 27 | 1.0949 | 69.12 | 0.5 % |
| 3 | 47.5700 | 4.36 | 21.76 % | 29 | 1.1539 | 77.28 | 0.51 % |
| 5 | 19.8382 | 16.68 | 9.07 % | 31 | 0.8513 | -77.61 | 0.38 % |
| 7 | 9.7368 | 5.45 | 4.45 % | 33 | 0.6986 | -65.81 | 0.31 % |
| 9 | 2.9590 | -60.06 | 1.35 % | 35 | 0.8136 | -57.95 | 0.37 % |
| 11 | 2.6503 | 87.87 | 1.21 % | 37 | 0.5224 | -29.30 | 0.24 % |
| 13 | 2.5124 | -72.39 | 1.15 % | 39 | 0.8271 | -30.61 | 0.38 % |
| 15 | 1.7850 | -53.44 | 0.82 % | 41 | 0.7655 | -8.06 | 0.35 % |
| 17 | 1.0888 | -41.71 | 0.5 % | 43 | 0.7048 | 17.62 | 0.32 % |
| 19 | 0.9919 | -16.91 | 0.45 % | 45 | 0.5357 | 55.14 | 0.24 % |
| 21 | 1.1165 | 8.91 | 0.51 % | 47 | 0.6428 | 74.92 | 0.29 % |
| 23 | 0.5885 | 4.54 | 0.27 % | 49 | 0.5676 | 89.23 | 0.26 % |
| 25 | 1.1472 | 64.33 | 0.52 % | 51 | 0.5676 | -89.23 | 0.26 % |

CONCLUSIONS

Due to difficulties arising from rich harmonics and un-availability of a standard design methodology shaded pole motors are mostly designed based on the trial-and-error method. The difficulty in the theoretical analysis stems from the existence of higher order harmonics with large amplitudes, which results from the existence of non-symmetrical windings in the stator and non-uniform air-gap profile. In this study, stator-rotor mutual inductance has been obtained by using the prepared test apparatus for the objective of obtaining a future equivalent circuit of the shaded pole motors with harmonics. Discrete Fourier analysis has been applied to obtain the mutual inductance waveform, and the harmonic components have been examined until the 51st harmonic. It has been seen that the 3rd, 5th, and 7th harmonics are very significant. The third harmonic is about 21.76% of the fundamental component. The main purpose of this study is to pave the way towards obtaining an effective equivalent circuit of the shaded pole motors, which should account for the harmonics. Towards this end, it is obvious that any future equivalent circuit should include equivalent circuit components for considering at least the 3rd, 5th, and 7th harmonic effects. With such an equivalent circuit, the performance of the shaded pole motors could be determined more precisely and will eliminate various alternative techniques appearing in the literature for this purpose.

ACKNOWLEDGMENT

This study was supported by Faneks Electric Motors Company. The authors thank them for their kind support.

REFERENCES

- Akbaba, M. & Fakhro, S. Q. 1992a.** An improved computational technique of the inductance parameters of the reluctance augmented shaded-pole motors using finite element method. *IEEE Transactions on Energy Conversion*, 7:308-314. DOI: 10.1109/60.136226.
- Akbaba, M. & Fakhro, S. Q. 1992b.** Field distribution and iron loss calculation in the reluctance augmented shaded pole motors using finite element method. *IEEE Transactions on Energy Conversion*, 7:302–307. DOI: 10.1109/60.136225.
- Bayram, D. & Mergen, A. F. 2009.** Investigation the effect of time harmonic in the asynchronous machine losses by finite element method. *EMO National Congress*, Ankara.
- Dalcalı, A. & Akbaba, M. 2016.** Comparison of 2D and 3D magnetic field analysis of single-phase shaded pole induction motors. *An International Journal Engineering Science and Technology*, 19:1-7. DOI: 10.1016/j.jestech.2015.04.013.
- Dehkordi, A. B. 2015.** A single-phase induction machine model for real-time digital simulation. *International Conference on Power Systems Transients*, Croatia.
- Gao, Y., Chau, K. T. & Ye, S. 2005.** A novel chaotic-speed single-phase induction motor drive for cooling fans. *14th IAS Annual Meeting Industry Application Conference*, Kowloon, Hong Kong. DOI: 10.1109/IAS.2005.1518553.
- Hajek, V., Mach, M. & Kuchar, L. 2015.** Special small electric motors. *International Conference on Electrical Drives and Power Electronics*, High Tatras. DOI: 10.1109/EDPE.2015.732509.
- Karmakar, A., Saha, P. K. & Panda, G. K. 2013.** D-q axis modelling analysis of a shaded pole induction motor and study of the non-linear behaviour. *International Conference on Power, Energy and Control*, Sri Rangalatchum Dindigul. DOI: 10.1109/ICPEC.2013.6527730.
- Kentli, F. 2009.** A survey on design optimization studies of induction motors during the last decade. *Journal of Electrical & Electronics Engineering Istanbul University*, 9:969-975.
- Kocabaş, D. A. & Mergen, A. F. 2006.** Contributions to reduce the effects of space harmonics in induction machines. *Itu Engineering journal-part d*, 2:25-36. URI: <http://hdl.handle.net/11527/10450>.
- Kocatepe, C., Uzunoglu, M., Yumurtacı, R., Karakas, A. & Arıkan, O. 2003.** *Harmonics in Electrical Installations*. Birsen Press. ISBN: 975-511-354-1.
- Liang, X., Faried, S. O. & El-Serafi, A. M. 2016.** Space harmonics of synchronous machines calculated by finite-element method. *IEEE Transaction on Industry Applications*, 52:1193-1203. DOI: 10.1109/ICPS.2015.7266428.
- Ojaghi, M. & Daliri, S. 2015.** A detailed dynamic model for single-phase shaded pole induction motors. *18th International Conference on Electrical Machines and Systems*, Pattaya. DOI: 10.1109/ICEMS.2015.7385366.
- Özçelik, N. G., Doğru, U. E. & Ergene, L. T. 2014.** Comparison study of drive motors for cooker hood applications. *16th International Power Electronics and Motion Control Conference and Exposition*, Antalya. DOI:10.1109/EPEPEMC.2014.6980684.

- Pop, A. A., Balan, H. & Radulescu, M. 2013.** Flux-density space-harmonics minimization for an axial-flux permanent-magnet machine. 4th International Symposium on Electrical and Electronics Engineering, Galati. DOI: 10.1109/ISEEE.2010.6674327.
- Sarac, V., Petkovska, L., Cundev, M. & Cvetkovski, G. 2005.** Comparison between two target functions for optimization of single phase shaded-pole motor using method of genetic algorithms. Journal of Materials Processing Technology, 161:89-95. DOI: 10.1016/j.jmatprotec.2004.07.010.
- Sarac, V. & Stefanov, G. 2011.** Calculation of electromagnetic fields in electrical machines using finite elements method. International Journal of Engineering and Industries, 26:21-29.
- Sarac, V. J., Stefanov, G. G. & Cvetkovski, V. 2010.** Influence of number of varied parameters on torque of single phase optimized motor models. 14th International IGTE Symposium on Numerical Fields Calculation in Electrical Engineering, Graz.

Submitted: 13/07/2016

Revised : 23/12/2016

Accepted : 25/12/2016